Experimental validation of rollout-based Model Predictive Control for Wave Energy Converters on a two-body, taut-moored point absorber prototype

Zechuan Lin, Xuanrui Huang, and Xi Xiao

Abstract—**Model predictive control (MPC) has proven its effectiveness in improving the energy capture efficiency of wave energy converters (WECs) subjected to physical constraints. A further step toward MPC's real-world application requires to speed up its online computation to meet the limited computational power of an industrial controller. To this end, an improved MPC method based on a rollout technique has been proposed, whose idea is to decouple the optimization and prediction horizons, so as to achieve long-horizon performance with short-horizon optimization. This rollout-based MPC has previously only been validated in simulation. In this study, it is put through wave tank testing and validated experimentally. A two-body, taut-moored point absorber prototype is constructed and the rollout-based MPC is implemented in real time. Experiment results confirm its energy efficiency as well as constraint satisfaction against the conventional MPC, and with this satisfactory performance its computational advantage is highlighted.**

Index Terms—**Wave Energy Converter, Model Predictive Control, Wave Tank Testing**

I. Introduction

In further reducing the levelized cost of energy for wave energy converters (WECs), advanced control can play a significant role [1]. For a typical point absorber WEC, the theoretical energy-maximizing condition can be derived in the frequency domain [2], and practical approximations such as the reactive control [3], latching [4], and velocity tracking [5] have been developed. Although simple and effective, these methods suffer from the incapability of handling various, device-specific constraints, such as the maximum displacement, generator force, and converter power. In the last decade, the dominant control solution for WECs is model predictive control (MPC), termed "the numerical era" [6]. At each execution step of MPC, the system trajectory during a finite future horizon is predicted using a mathematical model, based on which the control sequence that yields the highest energy output within constraints is solved with optimization. Then, the first control move is applied to the system, and the above process is repeated at the next step [7]. MPC has proven its effectiveness in addressing a variety of WEC constraints, such as uni-directional power flow and the operating range of an electric generator [8]. However, the real-world implementation of MPC faces the obstacle of online computation burden, since the optimizations need to be solved in real time, whereas the computation force of an industrial controller is limited.

One of the major approaches to speeding up computation is parameterization. In MPC, the optimization variable is a discrete sequence of control trajectory, whose dimension is typically high, since a long prediction horizon is necessary for satisfactory energy performance. By contrast, in methods like pseudospectral [9] and moment-based [10] parameterizations, the trajectory is represented by a combination of a set of base functions. In this way, the overall problem dimension can be reduced, but the optimization could also become nonlinear. In [11], an improved MPC is proposed based on a rollout technique inspired by artificial intelligence [12]. In this method, only a few control moves need to be solved, while the remaining trajectory is calculated by simulating a fixed control law termed the "rollout policy". By adopting a reactive control as the rollout policy, the problem can be maintained as quadratic programming. It has been shown by simulation case studies that long-horizon energy performance can be achieved with short-horizon optimization, so the computation burden is reduced considerably [11].

However, rollout-based MPC has not been implemented on a real WEC and validated experimentally. The necessity of experiments for WEC control can be highlighted in the following dilemma. On the one hand, real WEC systems, especially those to be deployed in the sea, are usually much more complex than the simulation environment. Effects that the widely-used linear hydrodynamic model cannot take into account include the nonlinear viscous force [13], the Coulomb-type mechanical friction [14], the mooring force [15] and the multiple degrees of freedom (DoF) motion [16]. On the other hand, practical control can only be based on simplified modeling to ensure its computational compactness in real time [6]. Hence, wave tank testing or even sea trails remain the ultimate standard for control validation. Recently, the WEC

This study was supported by the China National Key R&D Program under Grant 2020YFE0205400 and in part by the National Natural Science Foundation of China under Grant U1806224

The authors are with the Department of Electrical Engineering, Tsinghua University, Beijing 100084, China (Corresponding author: Xi Xiao, e-mail: xiao_xi@tsinghua.edu.cn)

Digital Object Identifier:
https://doi.org/10.36688/ewtec-2023-174

community has seen a number of experimental studies regarding advanced control, including a hardware-in-the-loop implementation [17], real-time MPC with wave tank testing [18] [19], and a linear time-invariant controller LiTe-Con [20] and its constraint-improved version LiTe-Con+ [21].

In this study, a novel WEC experimental platform is constructed. The device is a two-body, taut-moored point absorber similar to an actual application deployed in the sea [22]. This platform has unique features against the existing ones (e.g., the WaveStar prototype [20] and the heaving cylinder based on a fixed structure [19]) including the presence of a mooring system and multi-DoF motion and thereby stands as a good testing environment for control evaluation. Control-oriented modeling is applied and then both the conventional and rollout-based MPC are implemented and compared.

The contributions of this study are as follows. 1) Real-world performance of the rollout-based MPC is experimentally confirmed. 2) The effectiveness of simplified, control-oriented modeling of a complex WEC system is illustrated. 3) The concept of general approximate MPC, previously explored in [11] and [19], is further validated in terms of robustness against model mismatching, sub-optimality, and parameterization. 4) Finally, the successful demonstration gains unique engineering experience for the WEC community.

The remainder of this article is organized as follows. The WEC model and wave force estimation will be introduced in Section II. The conventional and rollout-based MPCs are proposed in Section III. The WEC prototype and control implementation are described in Section IV. The experimental results are presented in Section V.

II. WEC Model and Wave Force Estimation

A. Point Absorber Model

The dynamics of a single-body, heaving point absorber WEC can be described by

$$\begin{aligned}(M+M_\infty)\ddot{z}(t)+R_0\dot{z}(t)+\int_0^t h_r(t-\tau)\dot{z}(\tau)d\tau \\ +Kz(t)=w(t)+u(t),\end{aligned} \tag{1}$$

where t is continuous time; z, $\dot{z}$, and $\ddot{z}$ are the body's displacement, velocity, and acceleration, respectively; M is the body's mass; M_∞ is the infinite-frequency added mass; R_0 is the linear friction coefficient; h_r is the radiation impulse function; K is the buoyancy stiffness; w is the wave excitation force; and u is the PTO force.

By further representing the radiation kernel with a polynomial transfer function, establishing the continuous-time state space model, and discretizing this model with the zero-hold method of sampling time T_s, the following discrete-time model can be obtained

$$\mathbf{x}(k+1)=\mathbf{A}\mathbf{x}(k)+\mathbf{B}w(k)+\mathbf{B}u(k) \tag{2}$$

where k is the discrete time, $\mathbf{x}=[\dot{z},z,\mathbf{r}^{\mathrm{T}}]^{\mathrm{T}}\in\mathbb{R}^n$ is the system state with $\mathbf{r}\in\mathbb{R}^{n-2}$ being the radiation subsystem state, and $\mathbf{A}$, $\mathbf{B}$ are the system matrices. For their derivation, see [7].

B. Wave Excitation Force

The wave excitation force is originally an external input. But to estimate its value with techniques like the Kalman filter, it is now modeled as the sum of n_p sinusoidal components. Let the ith component be p_i, its derivative be $\dot{p}_i$, and its frequency be ω_i. So an additional state $\mathbf{p}=[p_1,\dot{p}_1,...,p_{n_p},\dot{p}_{n_p}]^{\mathrm{T}}$ including these components is incorporated in the system

$$\begin{aligned}\begin{bmatrix}\mathbf{x}(k+1)\\ \mathbf{p}(k+1)\end{bmatrix}&=\begin{bmatrix}\mathbf{A} & \mathbf{B}\mathbf{C}_\mathbf{p}\\ \mathbf{0} & \mathbf{A}_\mathbf{p}\end{bmatrix}\begin{bmatrix}\mathbf{x}(k)\\ \mathbf{p}(k)\end{bmatrix}+\begin{bmatrix}\mathbf{B}\\ \mathbf{0}\end{bmatrix}u(k)\\ \mathbf{y}(k)&=[\mathbf{C}\quad\mathbf{0}]\begin{bmatrix}\mathbf{x}(k)\\ \mathbf{p}(k)\end{bmatrix},\end{aligned} \tag{3}$$

where

$$\mathbf{A}_\mathbf{p}=\bigoplus_{i=1}^{n_p}\exp\left(T_s\begin{bmatrix}0 & 1\\ -\omega_i^2 & 0\end{bmatrix}\right),\ \mathbf{C}_\mathbf{p}=\mathbf{1}_{n_p}^{\mathrm{T}}\bigotimes[1,0] \tag{4}$$

where $\bigoplus$ and $\bigotimes$ denote the direct sum of matrices and the Kronecker product, respectively. The measurable signals of the system are the velocity and displacement, namely, $\mathbf{y}=[\dot{z},z]^{\mathrm{T}}$ and $\mathbf{C}=[\mathbf{I}_2,\mathbf{0}_{2\times(n-2+2n_w)}]$. Finally, by setting the noise parameters of the model and observation, the estimation of wave excitation force can be obtained using a classical linear Kalman filter (omitted here). This method is called Kalman filter with a harmonic oscillator (KFHO) [23]. The future wave forces can be predicted by a linear auto-regressive (AR) model, where the future values are modeled as linear combinations of historical values. The AR model has proven to be very suitable for ocean waves [6].

III. Model Predictive Control

A. Traditional Model Predictive Control

Let the maximum displacement and PTO force be z_m and u_m, respectively. The conventional MPC solves the following optimization at each step k:

$$\begin{aligned}\max_{u(k),...,u(k+N-1)}\quad & -\sum_{i=k}^{k+N-1}\frac{T_s}{2}u(i)(\mathbf{x}_1(i)+\mathbf{x}_1(i+1))\\ \text{s.t.}:\quad & \mathbf{x}(i+1)=\mathbf{A}\mathbf{x}(i)+\mathbf{B}u(i)+\mathbf{B}w(i),\\ & \qquad i=k,...,k+N-1\\ & -z_m\le\mathbf{x}_2(i)\le z_m,\quad i=k+1,...,k+N\\ & -u_m\le u(i)\le u_m,\quad i=k,...,k+N-1.\end{aligned} \tag{5}$$

where $\mathbf{x}_1$ and $\mathbf{x}_2$ denotes the velocity and displacement, respectively. In other words, at each step a control sequence $u(k),...,u(k+N-1)$ during a prediction horizon N is solved by maximizing the total output energy within constraints. The problem parameter is the observed state x and wave force information $w(k),...,w(k+N-1)$, and since the system is linear, this problem is a parametric quadratic program (pQP) as detailed in Appendix A.

B. Rollout-based Model Predictive Control

The rollout-based MPC [11] can be viewed as a parameterization of the original problem, where the prediction horizon N is separated into $N=N_1+N_2$; N_1 is the optimization horizon, which determines the

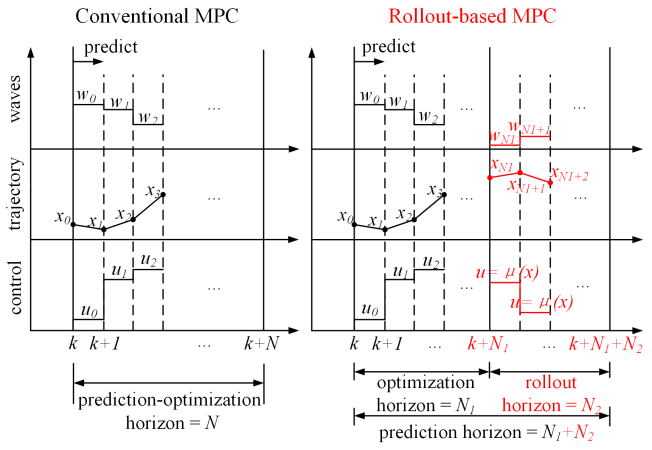

Fig. 1. Principles of conventional and rollout-based MPC methods

dimension of the final qQP, while N_2 is the rollout horizon, during which the PTO forces are calculated based on a fixed control law. The optimization of the rollout MPC can be described as

$$\begin{aligned}\max_{u(k),\ldots,u(k+N_1-1)} \; & -\sum_{i=k}^{k+N_1+N_2-1} \frac{T_s}{2} u(i)(\mathbf{x}_1(i)+\mathbf{x}_1(i+1)) \\ \text{s.t.}: \quad & \mathbf{x}(i+1)=\mathbf{A}\mathbf{x}(i)+\mathbf{B}u(i)+\mathbf{B}w(i), \\ & \qquad i=k,\ldots,k+N_1+N_2-1 \\ & -z_m \le \mathbf{x}_2(i) \le z_m, \quad i=k+1,\ldots,k+N_1 \\ & -u_m \le u(i) \le u_m, \quad i=k,\ldots,k+N_1-1 \\ & u(i)=\mu(\mathbf{x}(i)), \quad i=k+N_1,\ldots,k+N_1+N_2-1. \end{aligned} \tag{6}$$

where μ denotes the rollout policy. In other words, it is assumed that after N_1 steps, the system is controlled by μ for additional N_2 steps, and the optimal control sequence during the first N_1 steps is solved, such that the total energy during N_1+N_2 steps is maximized. Also, note that the constraints are imposed on the first N_1 steps only. The purpose of rollout is to decouple the prediction and optimization horizons, so as to achieve long-horizon energy performance with a small optimization dimension. The rollout policy is chosen as a reactive control as discussed in [11]. The qQP formulation is given in Appendix B. The principles of the two MPC formulations are illustrated in Fig. 1.

IV. Experiment Setup and Model Identification

A. WEC Prototype

The constructed point absorber prototype consists of a buoy and a spar. The buoy is floating on the water surface and oscillating with waves. The spar is semi-submerged and moored to a concrete block on the water floor through six mooring lines. The two bodies are connected through a ball screw, which is rigidly connected to a rotary generator. The device adopts a "taut-moored" design: the mooring lines are heavily pretensioned by letting the mass of the spar be much smaller than its buoyancy force. This design allows for much more effective force transmission from waves to the generator than a slack-moored device and thereby improves the power capture efficiency [22].

TABLE I
Key Parameters of the WEC Testing Platform

Part	Parameter	Value
Buoy	outer radius	0.75 m
	inner radius	0.15 m
	draft	0.3 m
	mass	508 kg
Spar	volume	1.2 m^3
	mass	745 kg
	length	2.85 m
	plate radius	1.6 m
Mooring	pretension	4795 N
	height	1.75 m

The structure of the device is depicted in Fig. 2. The design parameters are listed in Table I.

B. Installation

The experiment is conducted at the wave tank laboratory of the National Ocean Technology Center, Tianjin, China. The size of the tank is 100 m×18 m, and the water depth is 4.2 m. The device is fabricated and then installed in the wave tank as follows. First, it is transported to the wave tank by a bridge crane and lies flat on the water surface. Next, the concrete block is lifted from the bottom so that half of it is above the water. Then, the mooring chains are manually connected from the spar to the concrete block. Finally, the concrete block is slowly put down; during this process, it automatically drags the spar down and rotates the whole device to the normal position; in the meantime, the block itself automatically lies down on the bottom. The photo of the installed device is shown in Fig. 3.

Unlike some other platforms such as [24] where a structure is built to restrict the body motion to the heave direction, the position of the considered device is maintained only by the mooring system. Hence, in addition to the heave motion, there will also be surge and pitch motion when the body is excited by unidirectional waves.

C. Power Take-off and MPC Implementation

The PTO system consists of a permanent magnet synchronous generator (PMSG), an IGBT-based power

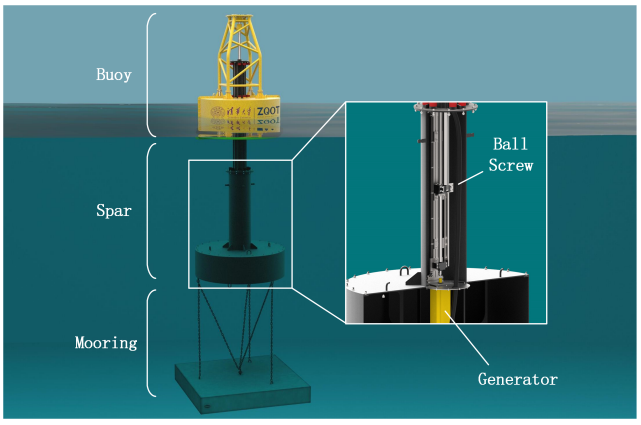

Fig. 2. Structure of two-body point absorber prototype

converter, and a bi-directional dc source. The control schematic is as follows: the MPC controller outputs a force command, this command is converted to the q-axis current command using field-oriented control (FOC) of the PMSG, and then a proportional-integral (PI) current loop is used to track this current command. The control algorithms are implemented on an NI PXIE controller with a sampling frequency of 10 kHz. The equipment is shown in Fig. 3, and the control diagram is shown in Fig. 4.

Both conventional and rollout-based MPCs are implemented. Control-oriented modeling [13] is applied, where the two-body, moored system is modeled as a single body oscillating in heave, and the parameters are calculated by the boundary element method (BEM) software NEMOH. The friction damping is identified separately. The prediction step size is 0.2 s. The optimization horizons are 30 (6 s) for the conventional MPC, covering two wave periods, and 4 (0.8 s) for rollout-based MPC, and the rollout horizon is 50 (10 s). The rollout-based MPC corresponds to a much-reduced computation burden. Due to the controller's computational limitation, the online solution of pQP adopts the fast-solving strategy [19], which involves the inheritance of the last solution, a feasible warm-start process, and a one-step, interior-point update. The MPC force command is updated at 100 Hz.

V. Results

A. Regular Waves

In each test case, waves are generated by a wave maker on the side of the tank. Then, we activate the control system and let the device run for up to five minutes. There should be several minutes between each test to wait for the water surface to recover. The maximum displacement is set to 0.1 m, while no constraint is imposed on the maximum force.

First, regular waves with a wave height of 0.2 m and a period of 3.0 s is tested, and the results are presented in Fig. 5 and Fig. 6. The following observations can be made from both figures: 1) the estimation of wave excitation force shows a quasi-sinusoidal waveform with certain oscillations, which are primarily due to model mismatch; 2) the body's velocity is generally in phase with the excitation force, which is an important indicator of wave power capture efficiency; 3) the displacement constraint is satisfied during the operation,

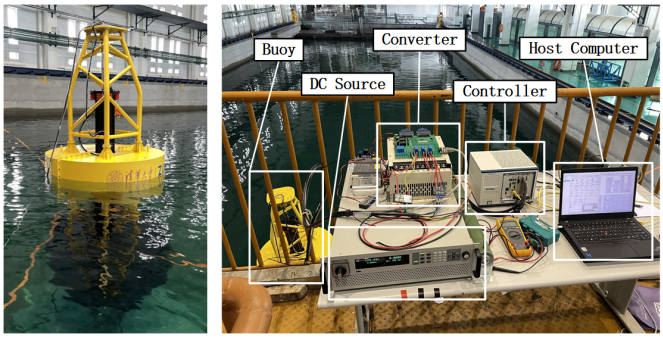

Fig. 3. Photo of point absorber prototype and electrical devices

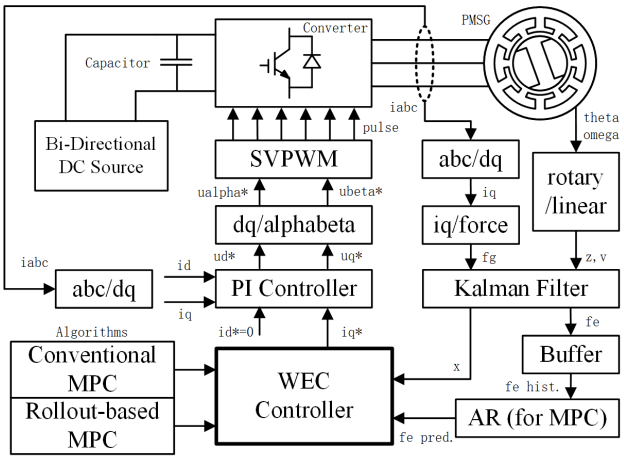

Fig. 4. Diagram of the WEC control system

as the buoy's motion is stopped by the controller and kept from violating the constraint when it is near the boundary; 4) the average powers (Pavg) are 38.5 W and 37.6 W, being very close. These observations confirm that the rollout-based MPC can achieve comparable control performance to conventional MPC with a very much reduced computation burden. Moreover, real-time MPC shows certain robustness against model mismatch and other disturbances, which can be explained by its receding-horizon nature as discussed in [11].

B. Irregular Waves

Then, irregular waves are generated with a JONSWAP spectrum with a significant wave height of 0.25 m and a peak period of 3.0 s, and the results are presented in Fig. 7 and Fig. 8. The following observations can be made: 1) under irregular waves, the control output by conventional MPC becomes more oscillating, while the rollout-based MPC performs more stable; 2) both methods remain successful in handling constraints; 3) the rollout-based MPC achieves slightly higher average power. The superiority in stability and efficiency against conventional MPC seems counter-intuitive since the rollout method in its nature is an approximation of the conventional, finite-horizon energy-maximizing control. One possible explanation is that due to the limited computation force in real time, the fast strategy [19] is adopted and only one interior-point iteration is carried out at each step. For the long-horizon optimization of conventional MPC, the quality of such an immature solution is more vulnerable to disturbances, whereas that of the short-horizon, rollout-based MPC is more robust.

VI. Conclusion

In this study, the rollout-based MPC proposed earlier is implemented on a two-body, taut-moored WEC prototype and put through wave tank testing. The rollout technique simulates the system trajectory with a reactive controller, so as to reduce the optimization horizon of MPC while maintaining its performance. The implementation of MPC is based on a fast-solving

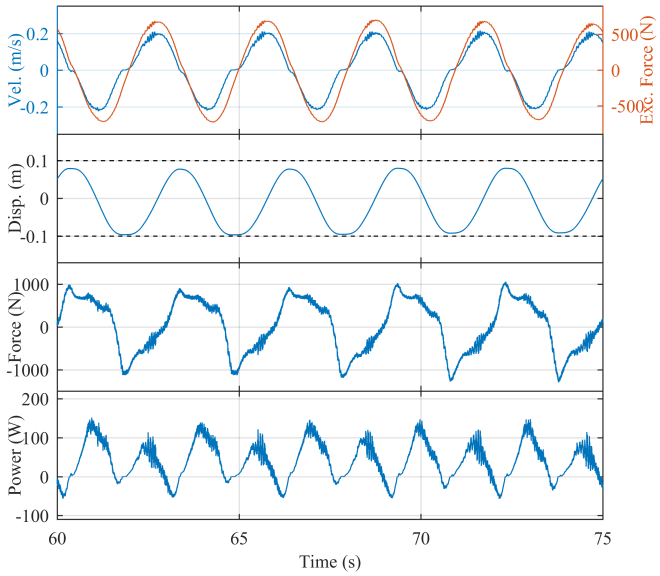

Fig. 5. Conventional MPC under regular waves, Pavg = 38.5 W

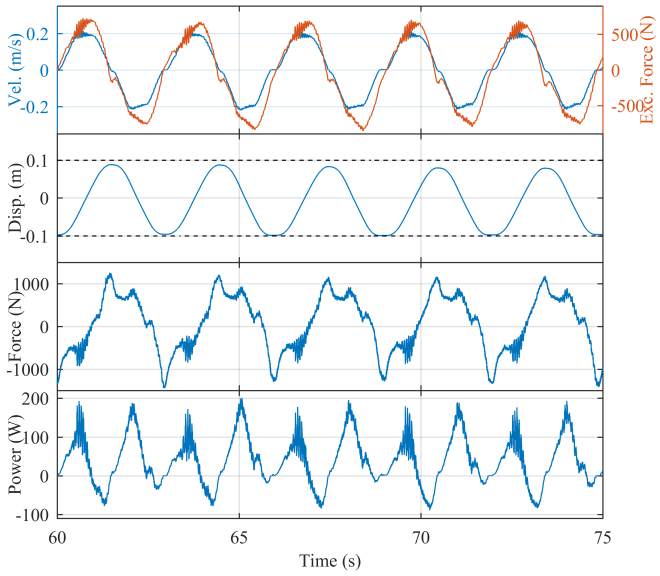

Fig. 6. Rollout-based MPC under regular waves, Pavg = 37.6 W

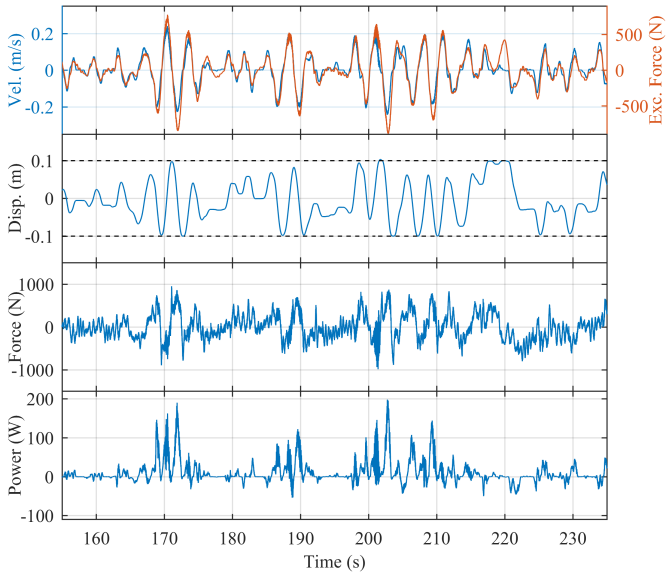

Fig. 7. Conventional MPC under irregular waves, Pavg = 10.5 W

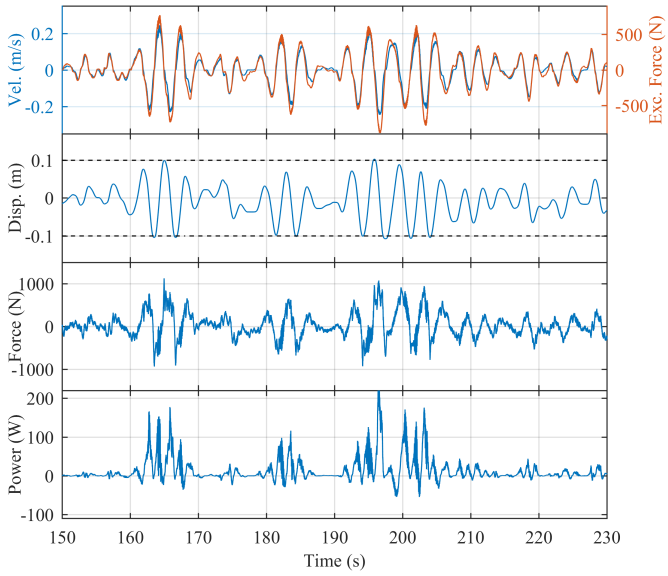

Fig. 8. Rollout-based MPC under irregular waves, Pavg = 13.3 W

strategy with a one-step interior-point method. The experimental results confirm that the rollout-based MPC can achieve comparable performance against the conventional MPC with significantly faster computation. Moreover, it is observed in our case that rollout-based MPC even shows better stability and higher efficiency under irregular waves.

APPENDIX A
FORMULATION OF TRADITIONAL MPC

Define $\mathbf{C_1} = [1, 0, \mathbf{0}_{n-2}^{\mathrm{T}}]$, $\mathbf{C_2} = [0, 1, \mathbf{0}_{n-2}^{\mathrm{T}}]$ and the following matrices for horizon i:

$$\frac{1}{2}\underbrace{\begin{bmatrix} 1 & & & \\ 1 & \ddots & & \\ \ddots & \ddots & & \\ & 1 & 1 & \end{bmatrix}}_{i+1} = \begin{bmatrix} \mathbf{\Phi_1}_{[i]} & \mathbf{\Phi_2}_{[i]} \end{bmatrix} = \begin{bmatrix} \frac{1}{2} & \mathbf{\Phi_{21}}_{[i]} \\ & \mathbf{\Phi_{22}}_{[i]} \end{bmatrix}$$

$$\mathbf{\Lambda_1}_{[i]} = \begin{bmatrix} \mathbf{C_1A} \\ \vdots \\ \mathbf{C_1A}^i \end{bmatrix}, \quad \mathbf{\Theta_1}_{[i]} = \begin{bmatrix} \mathbf{C_1B} & & \\ \vdots & \ddots & \\ \mathbf{C_1A}^{i-1}\mathbf{B} & \cdots & \mathbf{C_1B} \end{bmatrix}$$

$$\mathbf{\Lambda_2}_{[i]} = \begin{bmatrix} \mathbf{C_2A} \\ \vdots \\ \mathbf{C_2A}^i \end{bmatrix}, \quad \mathbf{\Theta_2}_{[i]} = \begin{bmatrix} \mathbf{C_2B} & & \\ \vdots & \ddots & \\ \mathbf{C_2A}^{i-1}\mathbf{B} & \cdots & \mathbf{C_2B} \end{bmatrix}$$

$$\mathbf{\Lambda_f}_{[i]} = \mathbf{A}^i, \qquad \mathbf{\Theta_f}_{[i]} = [\mathbf{A}^{i-1}\mathbf{B}, \cdots, \mathbf{B}]. \tag{7}$$

The following matrices can be derived:

$$\begin{aligned} \mathbf{H}_{[i]} &= \mathbf{\Phi_2}_{[i]}\mathbf{\Theta_1}_{[i]}, \\ \mathbf{G_x}_{[i]} &= \mathbf{\Phi_1}_{[i]} + \mathbf{\Phi_2}_{[i]}\mathbf{\Lambda_1}_{[i]}, \\ \mathbf{G_w}_{[i]} &= \mathbf{\Phi_2}_{[i]}\mathbf{\Theta_1}_{[i]}, \\ \mathbf{P}_{[i]} &= [\mathbf{\Theta}_{\mathbf{2}[i]}^{\mathrm{T}}, -\mathbf{\Theta}_{\mathbf{2}[i]}^{\mathrm{T}}, \mathbf{I}_i^{\mathrm{T}}, -\mathbf{I}_i^{\mathrm{T}}]^{\mathrm{T}}, \\ \mathbf{q_0}_{[i]} &= [z_m\mathbf{1}_i^{\mathrm{T}}, z_m\mathbf{1}_i^{\mathrm{T}}, u_m\mathbf{1}_i^{\mathrm{T}}, u_m\mathbf{1}_i^{\mathrm{T}}]^{\mathrm{T}}, \\ \mathbf{Q_x}_{[i]} &= [-\mathbf{\Lambda}_{\mathbf{2}[i]}^{\mathrm{T}}, \mathbf{\Lambda}_{\mathbf{2}[i]}^{\mathrm{T}}, \mathbf{0}_{n\times i}, \mathbf{0}_{n\times i}]^{\mathrm{T}}, \\ \mathbf{Q_w}_{[i]} &= [-\mathbf{\Theta}_{\mathbf{2}[i]}^{\mathrm{T}}, \mathbf{\Theta}_{\mathbf{2}[i]}^{\mathrm{T}}, \mathbf{0}_{i\times i}, \mathbf{0}_{i\times i}]^{\mathrm{T}} \end{aligned} \tag{8}$$

Let the prediction horizon be N. Let $\mathbf{u} = [u(k), ..., u(k+N-1)]^{\mathrm{T}}$ be the control sequence to be solved and $\mathbf{w}(k) = [w(k), ..., w(k+N-1)]^{\mathrm{T}}$ be the sequence of predicted wave excitation force. Then, the conventional MPC corresponds to the following pQP:

$$\begin{aligned} \min_{\mathbf{u}} \quad & \mathbf{u}^{\mathrm{T}}\mathbf{H}_{[N]}\mathbf{u} + (\mathbf{G}_{\mathbf{x}[N]}\mathbf{x}(k) + \mathbf{G}_{\mathbf{w}[N]}\mathbf{w}(k))^{\mathrm{T}}\mathbf{u} \\ \text{s.t.} \quad & \mathbf{P}_{[N]}\mathbf{u} \leq \mathbf{q}_{\mathbf{0}[N]} + \mathbf{Q}_{\mathbf{x}[N]}\mathbf{x}(k) + \mathbf{Q}_{\mathbf{w}[N]}\mathbf{w}(k). \end{aligned} \tag{9}$$

whose parameters are $\mathbf{x}(k)$ and $\mathbf{w}(k)$ obtained at the kth step. The problem dimension is N, which should be sufficiently large.

APPENDIX B
FORMULATION OF ROLLOUT-BASED MPC

Let $\mu(\mathbf{x}(k)) = R_g\mathbf{x}_1(k) + K_g\mathbf{x}_2(k)$ be the rollout policy, which is a reactive control law defined by R_g and K_g. Define $\mathbf{\Xi_0} = R_g\mathbf{C_1} + K_g\mathbf{C_2}$, $\mathbf{A_r} = \mathbf{A} + \mathbf{B\Xi_0}$, and the following matrices for horizon j:

$$\begin{aligned} \mathbf{\Lambda_{r1}}_{[j]} &= \begin{bmatrix} \mathbf{C_1A_r} \\ \vdots \\ \mathbf{C_1A_r}^{j} \end{bmatrix}, \mathbf{\Theta_{r1}}_{[j]} = \begin{bmatrix} \mathbf{C_1B} & & \\ \vdots & \ddots & \\ \mathbf{C_1A_r}^{j-1}\mathbf{B} & \cdots & \mathbf{C_1B} \end{bmatrix} \\ \mathbf{\Lambda_{r2}}_{[j]} &= \begin{bmatrix} \mathbf{C_2A_r} \\ \vdots \\ \mathbf{C_2A_r}^{j} \end{bmatrix}, \mathbf{\Theta_{r2}}_{[j]} = \begin{bmatrix} \mathbf{C_2B} & & \\ \vdots & \ddots & \\ \mathbf{C_2A_r}^{j-1}\mathbf{B} & \cdots & \mathbf{C_2B} \end{bmatrix} \\ \mathbf{\Xi_x}_{[j]} &= R_g\mathbf{\Lambda_{r1}}_{[j]} + K_g\mathbf{\Lambda_{r2}}_{[j]} \\ \mathbf{\Xi_w}_{[j]} &= R_g\mathbf{\Theta_{r1}}_{[j]} + K_g\mathbf{\Theta_{r2}}_{[j]} \end{aligned} \tag{10}$$

The following matrices can be derived:

$$\begin{aligned} \mathbf{H_{xx}}_{[j]} &= \mathbf{\Xi_0}^{\mathrm{T}}\left(\mathbf{C_1} + \mathbf{\Phi_{21}}_{[j]}\mathbf{\Lambda_{r1}}_{[j]}\right) + \mathbf{\Xi_x}_{[j]}^{\mathrm{T}}\mathbf{\Phi_{22}}_{[j]}\mathbf{\Lambda_{r1}}_{[j]} \\ \mathbf{G_{xw}}_{[j]} &= \mathbf{\Xi_0}^{\mathrm{T}}\mathbf{\Phi_{21}}_{[j]}\mathbf{\Theta_{r1}}_{[j]} + \mathbf{\Xi_x}_{[j]}^{\mathrm{T}}\mathbf{\Phi_{22}}_{[j]}\mathbf{\Theta_{r1}}_{[j]} \\ &\quad + \mathbf{\Lambda_{r1}}_{[j]}^{\mathrm{T}}\mathbf{\Phi_{22}}_{[j]}^{\mathrm{T}}\mathbf{\Xi_w}_{[j]} \\ \mathbf{H_f}_{[i,j]} &= \mathbf{\Theta_f}_{[i]}^{\mathrm{T}}\mathbf{H_{xx}}_{[j]}\mathbf{\Theta_f}_{[i]}, \\ \mathbf{G_{fx}}_{[i,j]} &= 2\mathbf{\Theta_f}_{[i]}^{\mathrm{T}}\mathbf{H_{xx}}_{[j]}\mathbf{\Lambda_f}_{[i]} \\ \mathbf{G_{fw1}}_{[i,j]} &= 2\mathbf{\Theta_f}_{[i]}^{\mathrm{T}}\mathbf{H_{xx}}_{[j]}\mathbf{\Theta_f}_{[i]}, \\ \mathbf{G_{fw2}}_{[i,j]} &= \mathbf{\Theta_f}_{[i]}^{\mathrm{T}}\mathbf{G_{xw}}_{[j]} \end{aligned} \tag{11}$$

Let the optimization horizon be N_1 and the rollout horizon be N_2, and $N_1 + N_2 = N$. Let $\mathbf{u_1} = [u(k), ..., u(k+N_1-1)]^{\mathrm{T}}$ be the control sequence to be solved and $\mathbf{w_1}(k) = [w(k), ..., w(k+N_1-1)]^{\mathrm{T}}$, $\mathbf{w_2}(k) = [w(k+N_1), ..., w(k+N_1+N_2-1)]^{\mathrm{T}}$ be the predicted wave excitation force sequences. Then, the rollout-based MPC corresponds to the following pQP:

$$\begin{aligned} \min_{\mathbf{u_1}} \quad & \mathbf{u_1}^{\mathrm{T}}\left(\mathbf{H}_{[N_1]} + \mathbf{H_f}_{[N_1,N_2]}\right)\mathbf{u_1} \\ & + \{(\mathbf{G_x}_{[N_1]} + \mathbf{G_{fx}}_{[N_1,N_2]})\mathbf{x}(k) \\ & + (\mathbf{G_w}_{[N_1]} + \mathbf{G_{fw1}}_{[N_1,N_2]})\mathbf{w_1}(k) \\ & + \mathbf{G_{fw2}}_{[N_1,N_2]}\mathbf{w_2}(k)\}^{\mathrm{T}}\mathbf{u_1} \\ \text{s.t.} \quad & \mathbf{P}_{[N_1]}\mathbf{u_1} \leq \mathbf{q_0}_{[N_1]} + \mathbf{Q_x}_{[N_1]}\mathbf{x}(k) + \mathbf{Q_w}_{[N_1]}\mathbf{w_1}(k). \end{aligned} \tag{12}$$

whose parameters are $\mathbf{x}(k)$, $\mathbf{w_1}(k)$ and $\mathbf{w_2}(k)$ obtained at the kth step. The problem dimension is N_1, which can be much smaller than N.

REFERENCES

[1] J. V. Ringwood, G. Bacelli, and F. Fusco, "Energy-maximizing control of wave-energy converters: The development of control system technology to optimize their operation," *IEEE Control Syst. Mag.*, vol. 34, no. 5, pp. 30–55, 2014.

[2] J. Falnes and A. Kurniawan, *Ocean waves and oscillating systems: linear interactions including wave-energy extraction*. Cambridge university press, 2020, vol. 8.

[3] X. Xiao, X. Huang, and Q. Kang, "A hill-climbing-method-based maximum-power-point-tracking strategy for direct-drive wave energy converters," *IEEE Trans. Ind. Electron.*, vol. 63, no. 1, pp. 257–267, 2015.

[4] W. Sheng, R. Alcorn, and A. Lewis, "On improving wave energy conversion, part ii: Development of latching control technologies," *Renewable Energy*, vol. 75, pp. 935–944, 2015.

[5] F. Fusco and J. V. Ringwood, "Hierarchical robust control of oscillating wave energy converters with uncertain dynamics," *IEEE Trans. Sustain. Energy*, vol. 5, no. 3, pp. 958–966, 2014.

[6] J. V. Ringwood, "Wave energy control: status and perspectives 2020," *IFAC-PapersOnLine*, vol. 53, no. 2, pp. 12 271–12 282, 2020.

[7] N. Faedo, S. Olaya, and J. V. Ringwood, "Optimal control, mpc and mpc-like algorithms for wave energy systems: An overview," *IFAC J. Syst. Control*, vol. 1, pp. 37–56, 2017.

[8] A. C. O'Sullivan and G. Lightbody, "Co-design of a wave energy converter using constrained predictive control," *Renewable Energy*, vol. 102, pp. 142–156, 2017.

[9] R. Genest and J. V. Ringwood, "Receding horizon pseudospectral control for energy maximization with application to wave energy devices," *IEEE Trans. Control Syst. Technol.*, vol. 25, no. 1, pp. 29–38, 2016.

[10] N. Faedo, Y. Peña-Sanchez, D. Garcia-Violini, F. Ferri, G. Mattiazzo, and J. V. Ringwood, "Experimental assessment and validation of energy-maximising moment-based optimal control for a prototype wave energy converter," *Control Eng. Practice*, vol. 133, p. 105454, 2023.

[11] Z. Lin, X. Huang, and X. Xiao, "A novel model predictive control formulation for wave energy converters based on the reactive rollout method," *IEEE Trans. Sustain. Energy*, vol. 13, no. 1, pp. 491–500, 2021.

[12] D. P. Bertsekas, *Reinforcement learning and optimal control*. Athena Scientific Belmont, MA, 2019.

[13] M. Farajvand, V. Grazioso, D. García-Violini, and J. V. Ringwood, "Uncertainty estimation in wave energy systems with applications in robust energy maximising control," *Renewable Energy*, vol. 203, pp. 194–204, 2023.

[14] B. Guo, R. Patton, S. Jin, J. Gilbert, and D. Parsons, "Nonlinear modeling and verification of a heaving point absorber for wave energy conversion," *IEEE Trans. Sustain. Energy*, vol. 9, no. 1, pp. 453–461, 2017.

[15] M. Richter, M. E. Magana, O. Sawodny, and T. K. Brekken, "Nonlinear model predictive control of a point absorber wave energy converter," *IEEE Trans. Sustain. Energy*, vol. 4, no. 1, pp. 118–126, 2012.

[16] O. Abdelkhalik, S. Zou, R. D. Robinett, G. Bacelli, D. G. Wilson, R. Coe, and U. Korde, "Multiresonant feedback control of a three-degree-of-freedom wave energy converter," *IEEE Trans. Sustain. Energy*, vol. 8, no. 4, pp. 1518–1527, 2017.

[17] A. S. Haider, T. K. Brekken, and A. McCall, "Real-time nonlinear model predictive controller for multiple degrees of freedom wave energy converters with non-ideal power take-off," *J. Mar. Sci. Eng.*, vol. 9, no. 8, p. 890, 2021.

[18] P. Tona, G. Sabiron, H.-N. Nguyen, A. Mérigaud, and C. Ngo, "Experimental assessment of the ifpen solution to the wec control competition," in *Int. Conf. Offshore Mechanics and Arctic Eng.*, vol. 84416. American Society of Mechanical Engineers, 2020, p. V009T09A023.

[19] Z. Lin, X. Huang, and X. Xiao, "Fast model predictive control system for wave energy converters with wave tank tests," *IEEE Trans. Ind. Electron.*, 2022.

[20] D. García-Violini, Y. Peña-Sanchez, N. Faedo, C. Windt, F. Ferri, and J. V. Ringwood, "Experimental implementation and validation of a broadband lti energy-maximizing control strategy for the wavestar device," *IEEE Trans. Control Syst. Technol.*, vol. 29, no. 6, pp. 2609–2621, 2021.

[21] D. García-Violini, Y. Peña-Sanchez, N. Faedo, F. Ferri, and J. V. Ringwood, "A broadband time-varying energy maximising control for wave energy systems (lite-con+): Framework and experimental assessment," *IEEE Trans. Sustain. Energy*, 2023.

[22] D. Elwood, S. C. Yim, J. Prudell, C. Stillinger, A. Von Jouanne, T. Brekken, A. Brown, and R. Paasch, "Design, construction, and ocean testing of a taut-moored dual-body wave energy

converter with a linear generator power take-off," *Renewable Energy*, vol. 35, no. 2, pp. 348–354, 2010.
[23] Y. Peña-Sanchez, C. Windt, J. Davidson, and J. V. Ringwood, "A critical comparison of excitation force estimators for wave-energy devices," *IEEE Trans. Control Syst. Technol.*, vol. 28, no. 6, pp. 2263–2275, 2019.
[24] D. Martin, X. Li, C.-A. Chen, K. Thiagarajan, K. Ngo, R. Parker, and L. Zuo, "Numerical analysis and wave tank validation on the optimal design of a two-body wave energy converter," *Renewable Energy*, vol. 145, pp. 632–641, 2020.